DALTON

Influence of anion on the solution and solid-state structures of some 1:2 adducts of silver(I) salts with 1,3-bis(diphenylphosphino)propane

Dermawan Affandi,[a] Susan J. Berners-Price,*,†,[b] Effendy,[a] Peta J. Harvey,[b] Peter C. Healy,[b] Beate E. Ruch[b] and Allan H. White[c]

[a] *Jurusam Pendidikan Kimia, FPMIPA IKIP Malang, Jalan Surabaya 6, Malang 65145, Indonesia*
[b] *Faculty of Science and Technology, Griffith University, Nathan, Brisbane, Queensland 4111, Australia*
[c] *Department of Chemistry, University of Western Australia, Nedlands, Western Australia 6907, Australia*

Crystallization of 1:2 silver(I) halide/pseudo halide:1,3-bis(diphenylphosphino)propane (dppp) mixtures from acetonitrile have resulted in the isolation of a novel series of neutral complexes, [AgX(dppp-*P*,*P*′)(dppp-*P*)] (X = Cl, Br, I or CN) containing co-ordinated anion and uni- and bi-dentate dppp ligands. In contrast, the thiocyanate and nitrate complexes precipitate as ionic [Ag(dppp-*P*,*P*′)$_2$]X with unco-ordinated anion and bidentate phosphine ligands, a structural type previously found for other 1:2 silver(I):diphosphine complexes. The complexes have been characterized by single-crystal X-ray structure determinations and solid-state ^{31}P cross-polarization magic angle spinning (CP MAS) NMR spectroscopy. The salt [Ag(dppp-*P*,*P*′)$_2$]SCN is obtained as crystals suitable for X-ray studies from pyridine, crystallizing as a sesqui-pyridine solvate in the monoclinic space group $P2_1/c$ with a = 10.691(2), b = 24.75(2), c = 22.360(4) Å, β = 108.38(1)°. The neutral $AgXP_3$ complexes (X = Cl, Br, I or CN) are isomorphous, crystallizing in the monoclinic space group $C2/c$, with $a \approx 21.8$, $b \approx 10.3$, $c \approx 45$ Å, β ≈ 95°. The solid-state ^{31}P CP MAS spectra are consistent with the structural results; the tetrahedral SCN and NO_3 complexes give a similar broad complex multiplet centred at δ −6, whereas the spectra of the neutral $AgXP_3$ complexes are interpretable as A_2BMX spin systems with signals assignable to the non-co-ordinated (δ −23), bidentate (δ *ca.* 13) and unidentate (δ *ca.* 3) phosphorus atoms. For the latter ^1J(P–Ag) couplings are in the range 288 Hz (CN) to 367 Hz (Br). Solution ^{31}P NMR studies on these complexes show that both neutral and ionic complexes exist in equilibrium in solution, with the position of the equilibrium dependent on the nature of the anion X. The potential significance to the antitumour activity of bis-chelated 1:2 silver(I)–diphosphine complexes is discussed.

Like their gold(I) counterparts, certain tetrahedral bis-chelated 1:2 silver(I)–diphosphine complexes of the type [Ag(P–P)$_2$]NO_3 [where P–P is $Ph_2P(CH_2)_2PPh_2$ (dppe), *cis*-$Ph_2PCH{=}CHPPh_2$ (dppey) or $Et_2P(CH_2)_2PEt_2$ (depe)] have been shown to exhibit antitumour activity against *i.p* P388 leukaemia in mice, as well as antifungal and modest antibacterial properties.[1,2] Although the mechanism for the cytotoxicity is not known, tumour cell mitochondria are likely targets for these lipophilic cations[3] and indeed, the complex [Ag(eppe)$_2$]NO_3 [where eppe is $Ph_2P(CH_2)_2PEt_2$] exhibits selective primary antimitochondrial activity in yeast.[4]

An understanding of the mechanisms responsible for the biological activity depends on a detailed knowledge of the different structural types that exist for silver(I) complexes of bidentate phosphines in the solid state and in solution. Tolazzi and co-workers have studied the thermodynamics of complexation of $Ag^{I}ClO_4$ with the bidentate phosphines $Ph_2P(CH_2)_nPPh_2$ (n = 1–3) in dimethyl sulfoxide[5] and propylene carbonate.[6] For n = 2 (dppe) and 3 (dppp) at 1:2 Ag:P–P ratios the only species present were ionic [Ag(P–P)$_2$]$^+$ complexes involving chelated diphosphine ligands. Similarly, in previous ^{31}P NMR studies[7] in chloroform solutions, only the bis-chelated ionic complexes [Ag(P–P)$_2$]NO_3 were observed for the bidentate phosphines dppe, dppp, depe, eppe and dppey; these had greatly enhanced kinetic and thermodynamic stabilities with respect to similar AgP_4 complexes containing monodentate phosphines, so that ^{109,107}Ag–^{31}P couplings were resolved in the ^{31}P NMR spectra at ambient temperatures.

† E-Mail: S.Berners-Price@sct.gu.edu.au

Both ClO_4^- and NO_3^- are non-co-ordinating anions; more relevant to biological systems are complexes of the type that exist in the presence of co-ordinating anions, particularly chloride. Both [Ag(dppe)$_2$]$^+$ and [Ag(eppe)$_2$]$^+$ cations (as nitrate salts) are stable in the presence of an excess of Cl^- ions,[1,4] indicating that chloride does not readily displace phosphorus from the Ag^{I} co-ordination sphere. Of great interest therefore is a novel class of compounds that we have isolated for 1:2 adducts of a number of silver(I) compounds, AgX, with dppp in the context of systematic studies of AgX:dppx type adducts.[8] For X = Cl, Br, I or CN in the solid state the compounds exist as neutral complexes of type [AgX(dppp-*P*,*P*′)(dppp-*P*)] with both uni- and bi-dentate dppp ligands and co-ordinated anion. In contrast, the thiocyanate complex is not of this type but, rather, ionic [Ag(dppp)$_2$]SCN.

We report here the characterization of these compounds by single-crystal X-ray structure determinations and compare the structures that exist in the solid state to those in solution by comparison of results from solid state ^{31}P cross-polarization magic angle spinning (CP MAS) and solution ^{31}P NMR spectroscopy. We show that the extent of dissociation of the complexes in solution to form cationic [Ag(dppp)$_2$]$^+$ and/or other species depends critically on the nature of the anion X.

Experimental

Preparation of compounds

[AgX(dppp-*P*,*P*′)(dppp-*P*)] (X = Cl, Br, I or CN). All compounds were prepared similarly. The compounds AgX (1.0 mmol) and dppp (0.85 g, 2.1 mmol) were dissolved with warm-

ing in acetonitrile (*ca.* 20 cm^3). After filtration, the solutions were allowed to stand and cool, depositing colourless crystals of the product. X = Cl: m.p. 124–126 °C (Found: C, 66.8; H, 5.5. $C_{54}H_{52}AgClP_4$ requires C, 67.0; H, 5.4%). X = Br: m.p. 147–149 °C (Found: C, 63.9; H, 5.2. $C_{54}H_{52}AgBrP_4$ requires C, 64.05; H, 5.2%). X = I: m.p. 159–161 °C (Found: C, 61.4; H, 5.1. $C_{54}H_{52}AgIP_4$ requires C, 61.2; H, 4.95%). X = CN: m.p. 115–117 °C (Found: C, 68.9; H, 5.4; N, 1.6. $C_{55}H_{52}AgNP_4$ requires C, 68.9; H, 5.45; N, 1.45%).

$[Ag(dppp)_2]SCN·1.5py$ (py = pyridine). With AgSCN the same procedure as for the halide and CN compounds yielded a white precipitate. This was dissolved in warm pyridine (*ca.* 5 cm^3) giving a clear solution, which on cooling deposited colourless crystals, m.p. 95–97 °C (Found: C, 67.8; H, 5.3; N, 3.0; S, 3.0. $C_{62.5}H_{59.5}AgN_{2.5}P_4S$ requires C, 67.65; H, 5.4; N, 3.2; S, 2.9%).

$[Ag(dppp)_2]NO_3$. This was prepared essentially according to the literature method,[7] by addition of $AgNO_3$ (0.085 g, 0.5 mmol) in water (10 cm^3) to a solution of dppp (0.42 g, 1 mmol) in acetone (20 cm^3). Colourless microcrystalline material formed from the clear solution on standing.

Crystallography

Structure determinations. Unique room temperature diffractometer data sets (Enraf-Nonius CAD-4 instrument, $T \approx 295$ K, monochromatic Mo-Kα radiation $\lambda = 0.710\,73$ Å) were measured to $2\theta_{max} = 50°$ yielding N independent reflections, N_o with $I > 3\sigma(I)$ being considered 'observed' and used in the full-matrix least-squares refinements after Gaussian absorption corrections. Anisotropic thermal parameters were refined for the non-hydrogen atoms, $(x,y,z,U_{iso})_H$ being included constrained at estimated values. Conventional residuals (on $|F|$), R and R' are quoted, statistical reflection weights being derivative of $\sigma^2(I) = \sigma^2(I_{diff}) + 0.0004\sigma^4(I_{diff})$. Neutral-atom complex scattering factors were employed, computation using the XTAL 3.2 program system implemented by S. R. Hall.[9] Pertinent results are given in the figures and tables. Abnormal features/variations in procedures/comments for individual samples are recorded below ('Variata'). In all figures 20% thermal ellipsoids are shown for the non-hydrogen atoms; hydrogen atoms, where included, have arbitrary radii of 0.1 Å.

Atomic co-ordinates, thermal parameters, and bond lengths and angles have been deposited at the Cambridge Crystallographic Data Centre (CCDC). See Instructions for Authors, *J. Chem. Soc., Dalton Trans.*, 1997, Issue 1. Any request to the CCDC for this material should quote the full literature citation and the reference number 186/412.

Crystal data. The compounds $[AgX(dppp)_2]$ (X = Cl, Br, I or CN) are isomorphous, monoclinic, space group $C2/c$ (C_{2h}^6, no. 15), $Z = 8$.

X = Cl. $C_{54}H_{52}AgClP_4$, $M = 968.3$, $a = 21.731(9)$, $b = 10.26(1)$, $c = 44.61(2)$ Å, $\beta = 94.44(4)°$, $U = 9917$ Å^3, $D_c = 1.30$ g cm^{-3}, $F(000) = 4000$, $\mu_{Mo} = 6.2$ cm^{-1}, crystal size 0.22 × 0.46 × 0.16 mm, $A^*_{min,max} = 1.09, 1.13$, $N = 8718$, $N_o = 2911$, $R = 0.065$, $R' = 0.069$.

X = Br. $C_{54}H_{52}AgBrP_4$. $M = 1012.7$, $a = 21.709(5)$, $b = 10.289(5)$, $c = 44.920(9)$ Å, $\beta = 94.76(2)°$, $U = 9998$ Å^3, $D_c = 1.35$ g cm^{-3}, $F(000) \approx 4144$, $\mu_{Mo} = 13.6$ cm^{-1}, crystal size 0.23 × 0.42 × 0.05 mm, $A^*_{min,max} = 1.06, 1.32$, $N = 7628$, $N_o = 2697$, $R = 0.067$, $R' = 0.071$.

X = I. $C_{54}H_{52}AgIP_4$, $M = 1059.7$, $a = 21.77(1)$, $b = 10.341(8)$, $c = 45.35(2)$ Å, $\beta = 95.51(4)°$, $U = 10\,162$ Å^3, $D_c = 1.39$ g cm^{-3}, $F(000) = 4288$, $\mu_{Mo} = 10.6$ cm^{-1}, crystal size 0.20 × 0.42 × 0.16 mm, $A^*_{min,max} = 1.17, 1.24$, $N = 8945$, $N_o = 4514$, $R = 0.041$, $R' = 0.041$.

X = CN. $C_{55}H_{52}AgNP_4$, $M = 958.8$, $a = 21.892(9)$, $b = 10.257(9)$, $c = 44.68(2)$ Å, $\beta = 94.36(3)°$, $U = 10\,003$ Å^3, $D_c = 1.27$ g cm^{-3}, $F(000) = 3968$, $\mu_{Mo} = 5.7$ cm^{-1}, crystal size 0.26 × 0.42 × 0.10 mm, $A^*_{min,max} = 1.05, 1.19$, $N = 7443$, $N_o = 3334$, $R = 0.065$, $R' = 0.072$.

Variata. All compounds presented common problems associated with (*a*) the long *c* axis (possibly introducing some systematic error by way of uncompensated reflection overlap, despite the use of an extended counter arm), (*b*) rather weak data and (*c*) disorder in the terminal phosphorus of the unidentate dppp ligand, and, less well defined and unresolved, its neighbouring atoms; phosphorus populations x, $(1 - x)$ refined to $x = 0.77(1)$, 0.84(1), 0.899(5), 0.85(1) for the four compounds. Inter-component P···P distances are 1.74(3), 1.76(4), 1.67(2) and 1.76(3) Å, respectively; the location of the second component (Fig. 2) corresponds more plausibly to that expected for inversion of the phosphorus [as in one of the phases of trimesitylphosphine[10] in which the two sites are 1.725(6) Å apart] rather than, for example, the full or partial occupancy of an associated oxygen site of any oxide impurity should it be present. No resonances for phosphine oxide were discernible in the solid-state CP MAS ^{31}P NMR spectra of these complexes. ω Scans were used for data measurement.

$[Ag(dppp)_2]SCN·1.5py$. $C_{55}H_{52}AgNP_4S·1.5C_5H_5N$, $M = 1109.5$. Monoclinic, space group $P2_1/c$ (C_{2h}^5, no. 14), $a = 10.691(2)$, $b = 24.75(2)$, $c = 22.360(4)$ Å, $\beta = 108.38(1)°$, $U = 5614$ Å^3, D_c ($Z = 4$) = 1.31 g cm^{-3}, $F(000) = 2300$, $\mu_{Mo} = 5.5$ cm^{-1}, crystal size 0.51 × 0.28 × 0.16 mm, $A^*_{min,max} = 1.09, 1.16$, $N = 9087$, $N_o = 5083$, $R = 0.052$, $R' = 0.051$.

Variata. 2θ/θ Scan mode. Pyridine thermal motion is high; solvent(2) is disposed about an inversion centre with modelling of the nitrogen, tentatively assigned, as disordered.

NMR Spectroscopy

Solid-state CP MAS ^{31}P NMR spectra were obtained at ambient temperature on a Varian UNITY-400 spectrometer at 161.92 MHz. Single contact times of 2 ms were used with a proton pulse width of 7.0 μs, a proton decoupling field of 62 kHz and a recycle delay time of 30 s. The samples were packed in Kel-F inserts within silicon nitride rotors and spun at a speed of 5 kHz at the magic angle. Between 60 and 200 free induction decays were collected and transformed with experimental line broadening values of 10–20 Hz. The ^{31}P CP MAS two-dimensional correlation (COSY) experiment was recorded using the pulse sequence[11] available in the Varian Solids User Library, and use of the Haberkorn–Ruben (hypercomplex) method for pure-phase quadrature detection in the F1 dimension. The contact time, ^{1}H 90° pulse length and spin-rate were the same as those implemented in the one-dimensional experiment. Typically a total of 200–256 time increments were used in each of which 64 transients were added, with a 5 s recycle delay. Both dimensions were zero-filled to 1 K words and weighted with sine-bell apodization prior to Fourier transformation. Chemical shift data are referenced to 85% H_3PO_4 *via* an external sample of solid PPh_3 (δ −9.9). Solution ^{31}P NMR spectra were recorded on the same instrument on samples dissolved in $CDCl_3$ or CH_2Cl_2–10% CD_2Cl_2 (3 cm^3) in 10 mm NMR tubes at variable temperatures (297–183 K). Spectra consisting of 8000 data points were acquired using an 8 μs (45°) pulse, proton Waltz decoupling and a 1 s relaxation delay. A total of 256 scans were collected and the spectra processed with a 1–5 Hz line broadening. The chemical shifts were referenced to external 85% H_3PO_4 (δ 0) measured at 295 K.

Results and Discussion

Crystal structures

The results of the room-temperature single-crystal X-ray studies are consistent with the formulation of the complexes, in terms of stoichiometry and connectivity, as 1:2 AgX:dppp adducts (X = Cl, Br, I, CN or SCN); in all cases, one formula

Table 1 Molecular core geometries (angles in °) for $[Ag(dppp)_2]SCN\cdot 1.5py$. Ligand angles (values for ligands a, b respectively)

Ag–P(1)–C(1)	111.6(3), 110.4(2)	Ag–P(2)–C(2)	111.8(2), 110.6(2)
P(1)–C(1)–C(12)	115.8(5), 116.2(5)	P(2)–C(2)–C(12)	113.1(5), 116.4(5)
C(1)–C(12)–C(2)	114.6(7), 115.6(6)		
Ag–P(1)–C(111)	121.0(3), 121.5(2)	Ag–P(2)–C(211)	111.5(3), 121.3(2)
Ag–P(1′)–C(121)	113.0(2), 114.9(2)	Ag–P(2)–C(221)	120.3(2), 113.5(3)
C(1)–P(1)–C(111)	103.2(3), 102.4(3)	C(2)–P(2)–C(211)	104.5(8), 103.2(3)
C(1)–P(1)–C(121)	102.5(3), 101.8(4)	C(2)–P(2)–C(221)	101.5(3), 102.8(3)
C(111)–P(1)–C(121)	103.6(3), 103.3(3)	C(211)–P(2)–C(221)	105.8(3), 103.3(3)
P(2)–Ag–P(1)–C(1)	−25.7(2), −31.7(3)	P(1)–Ag–P(2)–C(2)	29.1(3), 32.6(3)
Ag–P(1)–C(1)–C(12)	50.3(6), 54.9(6)	Ag–P(2)–C(2)–C(12)	−56.6(5), −57.2(6)
P(1)–C(1)–C(12)–C(2)	−82.1(7), −79.7(8)	P(2)–C(2)–C(12)–C(1)	85.4(6), 81.3(7)
P(2)–Ag–P(1)–C(111)	−147.4(2), −151.6(3)	P(1)–Ag–P(2)–C(211)	145.6(2), 153.4(3)
P(2)–Ag–P(1)–C(121)	89.1(3), 82.9(3)	P(1)–Ag–P(2)–C(221)	−89.8(3), −82.4(3)
Ag–P(1)–C(111)–C(112)	81.7(7), −105.1(6)	Ag–P(2)–C(211)–C(212)	−103.9(6), 160.9(5)
Ag–P(1)–C(121)–C(122)	17.7(7), −167.6(6)	Ag–P(2)–C(221)–C(222)	−11.6(8), 55.5(6)

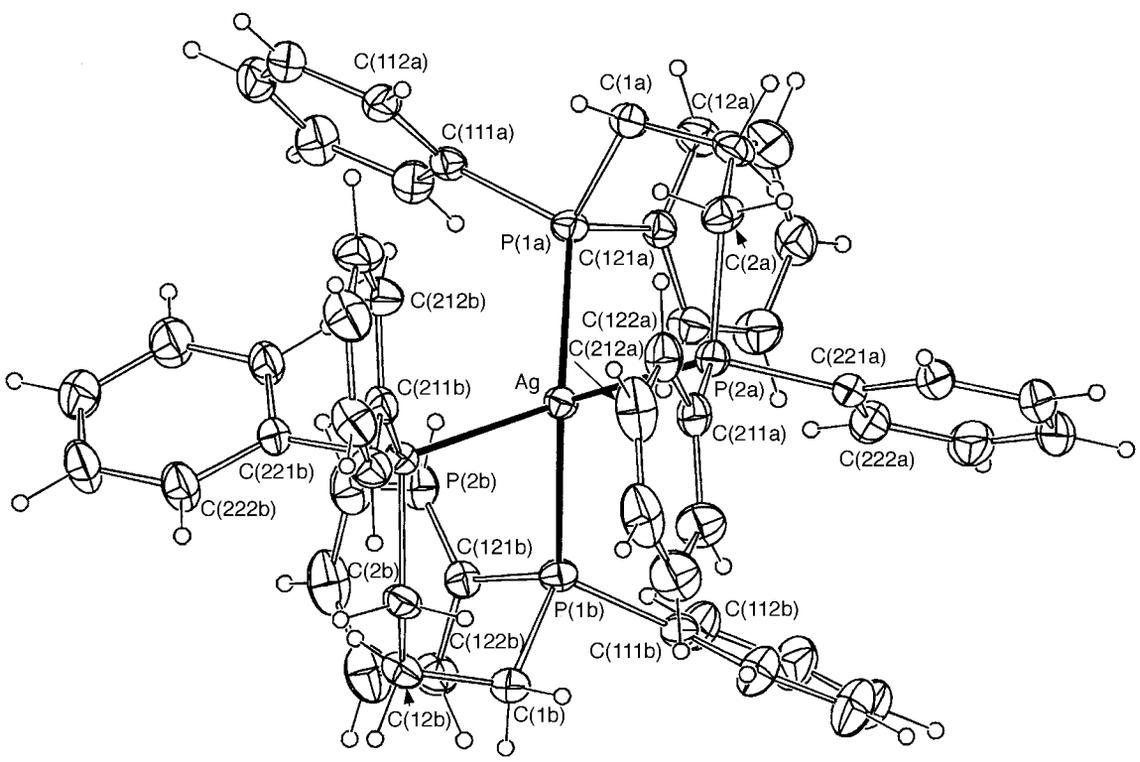

Fig. 1 Projection of the $[Ag(dppp)_2]^+$ cation of the thiocyanate complex down its quasi-2 axis

unit comprises the asymmetric unit of the structure, with four-co-ordinate silver(I) atoms. The thiocyanate complex obtained from pyridine solution is ionic, $[Ag(dppp)_2]^+(SCN)^-$ as a pyridine sesqui-solvate. The $[Ag(dppp)_2]^+$ cation represents the first bis[bidentate bis(diphenylphosphino)propane]silver(I) cation structurally characterized. The pyridine appears to have no unusual interactions with cation or anion, but simply occupies lattice voids, with high thermal motion, also evident on the anion and rendering insignificant the recorded geometries of these moieties. The cation has quasi-2, non-crystallographic symmetry, closely approximated by ring torsions (Table 1) and phenyl ring dispositions about one pole; about the other, the relation is more approximate (Fig.1). The bite angles of the two ligands are similar, while interligand P–Ag–P angles about the quasi-symmetry axis are appreciably different: 108.83(7) *vs.* 120.34(7)° reflecting a lowering of the symmetry of the complex from D_{2d}. A slight asymmetry in the Ag–P distances is observed for each ligand with differences of ≈0.03 and ≈0.01 Å for ligands a and b, respectively. The structure of this cation can be compared to the three other reported structures in which silver(I) is bis-chelated by two bidentate diphenylphosphine ligands:[12–14] $[Ag(dppe)_2]NO_3$, $[Ag(dppey)_2][Ph_3Sn(NO_3)_2]$ and $[Ag(dppf)_2]ClO_4$ [where dppf is 1,1′-bis(diphenylphosphino)-ferrocene]. Comparative data are presented in Table 2. For all of these structures, the $[Ag(P–P)_2]$ geometry is only slightly distorted from D_{2d} symmetry with the angles[15] θ_x, θ_y, θ_z close to the expected values of 90° (Table 2). The mean Ag–P distances vary from 2.473(7) for $[Ag(dppey)_2][Ph_3Sn(NO_3)_2]$ to 2.57(2) Å for $[Ag(dppf)_2]ClO_4$, with the value of 2.52(2) Å for the present dppp complex similar to that recorded for $[Ag(dppe)_2]NO_3$. These results can be compared also with data obtained for complexes containing the $[Ag(PPh_3)_4]^+$ cation where for example, for the nitrate complex,[16] the Ag–P bond lengths are 2.643(3) (×3) and 2.671(4) Å, with P–Ag–P angles close to the tetrahedral angle.

In the Cl, Br, I and CN, complexes, the silver atom is also bonded to two dppp ligands within a discrete mononuclear species but, unlike the SCN complex, one of these is unidentate rather than bidentate, the fourth co-ordination site being occupied by the halide or cyanide group to give a neutral $AgXP_2P$ molecule (Fig. 2). The P–Ag–P angle within the bidentate ligand is the smallest angle within the co-ordination sphere,

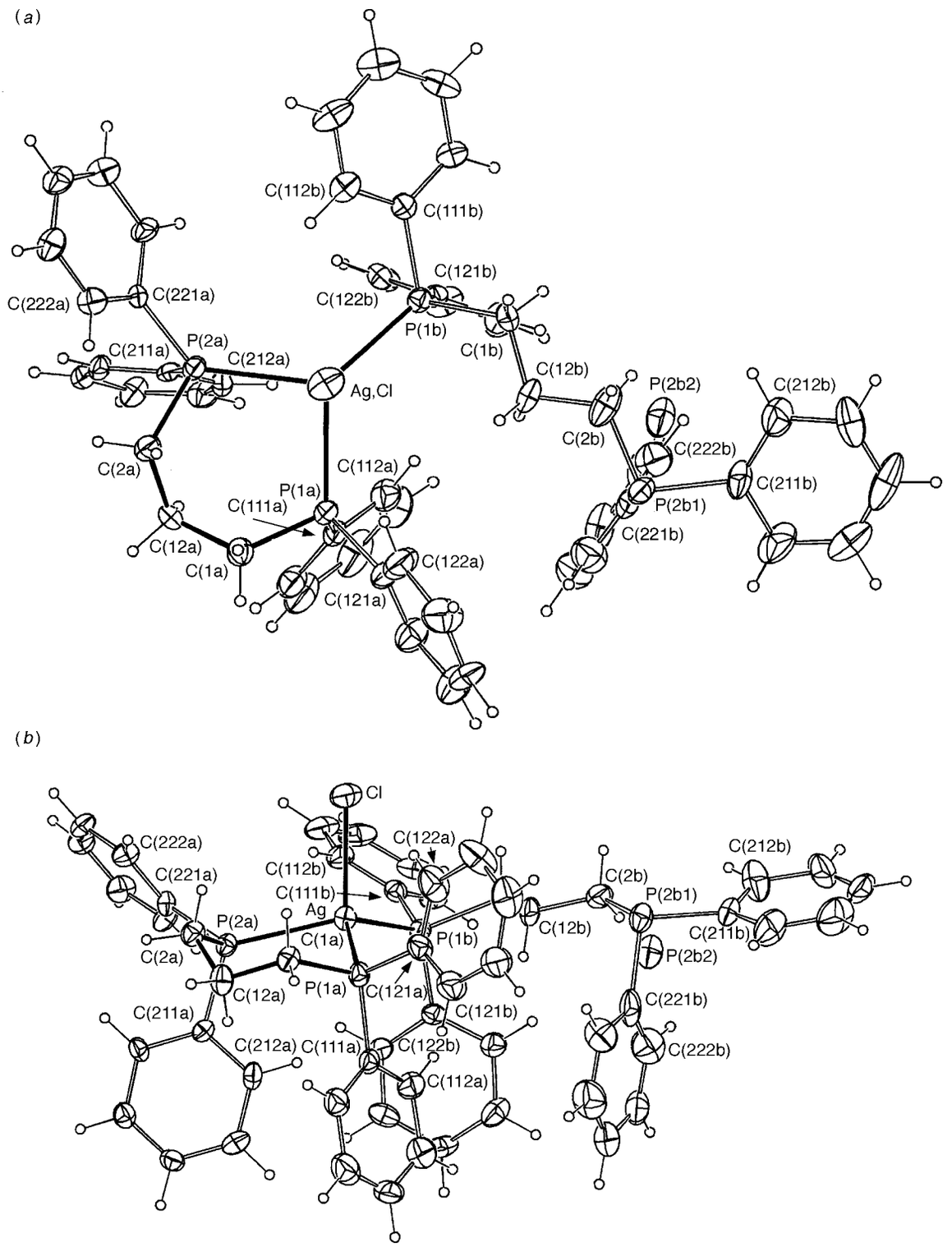

Fig. 2 Projection of [AgCl(dppp-*P*,*P*′)(dppp-*P*)] (*a*) down and (*b*) normal to the Cl–Ag bond; the disordered P(2b) component is included in both

and not noticeably different from the values observed in those of the cation arrays; the ring conformation has approximate *m* symmetry here, with phosphorus substituents equatorial and axial, the latter to the same side of the ligands (Table 3). The Ag–P (bidentate) bond lengths are also similar, but Ag–P (unidentate), in a more spacious disposition, is shorter. The X–Ag–P angles are similar in magnitude, the P (unidentate)–Ag–P (bidentate) angles being the largest. In all bidentate ligands, angles within the rings are quasi-tetrahedral at the phosphorus and larger at the carbon atoms. About the metal centre minor geometrical differences only are found between Cl, Br and I adducts; the geometry of the cyanide adduct deviates more substantially, Ag–P being elongated by *ca.* 0.02 Å for the bidentate and 0.03_5 Å for the unidentate ligand, with the X–Ag–P angle also enlarged, all indicative of increased Ag–X interaction in the cyanide (Table 3). The $[AgX(PPh_3)_3]$ analogues, considered in comparison, exist in a wide variety of phases;[12,17] Ag–P bond lengths in the chloride and bromide complexes usually lie in the range 2.54–2.60 Å; one of the ligands is incipiently dissociating in the iodide and cyanide, with one Ag–P bond 0.2 (X = I) to 0.5 Å (X = CN) longer than the other two. The Ag–X bond lengths in these complexes are similar to those found for the present series, differences being of the order of 2% or less.

Table 2 Comparative core geometries (distances in Å, angles in °) for tetrahedral $[Ag(P{-}P)_2]X$ complexes[a]

	dppe[b]	dppey[c]	dppp[d]	dppf[e]
Ag–P(1a)	2.488(3)	2.472(2)	2.527(2)	2.561(2)
Ag–P(2a)	2.523(3)	2.476(2)	2.501(3)	2.584(2)
Ag–P(1b)	2.527(3)	2.479(2)	2.526(2)	2.549(2)
Ag–P(2b)	2.523(3)	2.463(2)	2.516(2)	2.602(2)
⟨Ag–P⟩	2.51(2)	2.473(7)	2.52(2)	2.57(2)
P(1a)–Ag–P(2a)	84.5(1)	84.1(1)	93.51(7)	105.71(4)
P(1a)–Ag–P(1b)	129.5(1)	123.8(1)	120.34(7)	113.15(4)
P(1a)–Ag–P(2b)	128.8(1)	127.8(1)	122.99(6)	117.84(4)
P(2a)–Ag–P(1b)	116.0(1)	117.8(1)	120.65(6)	106.81(4)
P(2a)–Ag–P(2b)	117.9(1)	124.2(1)	108.83(7)	114.54(4)
P(1b)–Ag–P(2b)	83.8(1)	83.9(1)	92.39(7)	98.39(4)
θ_x	89.8	85.7	86.7	86.0
θ_y	100.3	94.0	96.2	94.6
θ_z	91.3	91.5	96.5	91.4

[a] θ_z is generally similar to the dihedral angle between ligand planes usually reported for this type of structure. For molecules adopting D_{2d} symmetry, $\theta_x = \theta_y = \theta_z = 90.0°$. Deviation of θ_z from 90° represents a 'twisting' of ligand b relative to ligand a and lowers the symmetry to D_2. Values of θ_x and θ_y different from 90° represent 'rocking' or 'waggling' displacements of ligand b with respect to ligand a (ref. 15). [b] Ref. 12, X = NO_3. [c] Ref. 13, X = $Ph_3Sn(NO_3)_2$. [d] This work, X = SCN. In the anion, C–S,N are 1.76(1), 0.68(1) Å; S–C–N is 164(1) Å. [e] Ref. 14, X = ClO_4.

Solid-state ^{31}P NMR spectroscopy

The ^{31}P CP MAS solid-state spectra of the complexes $[Ag(dppp)_2]X$ (X = NO_3 or SCN) and [AgX(dppp-*P*,*P*′)(dppp-*P*)] (X = Cl, Br, I or CN) are shown in Fig. 3. The spectrum of the SCN complex, precipitated from acetonitrile solution, consists principally of a complex multiplet centred at δ −6 [Fig. 3(*b*)]; the ^{31}P chemical shift is in a similar region to that of $[Ag(dppp)_2]^+$ in solution (Fig. 5), but in the solid state the four P atoms are crystallographically distinct, resulting in magnetic inequivalence and hence a more complex multiplet pattern is expected. The spectrum of the nitrate complex [Fig. 3(*a*)] is almost identical to that of the SCN complex, showing that the multiplet pattern is independent of the anion. However, recrystallization of the SCN complex from pyridine resulted in small changes in the appearance of the ^{31}P CP MAS multiplet (not shown), with further distinct peaks observable at δ *ca.* −3 and +1, the intensities of which were dependent on the conditions of crystallization. This is suggestive of the presence of different phases of $[Ag(dppp)_2]^+$, possibly as a consequence of variation in lattice site occupancy by the pyridine solvent.

The solid-state ^{31}P CP MAS spectra of the four neutral [AgX(dppp-*P*,*P*′)(dppp-*P*)] complexes are similar [Fig. 3(*c*)–3(*f*)], and distinct from those of the ionic bis-chelated complexes, consisting of three distinct sets of ^{31}P resonances: a broad high-field singlet (δ −23), a broad low-field doublet (δ *ca.* −3) and an intermediate multiplet (δ *ca.* −13) whose appearance is anion dependent. These spectral results are consistent with the structural data with the high-field singlet and low-field doublet assignable to the terminal and co-ordinated phosphorus atoms of the unidentate dppp ligand, respectively, and the complex multiplet at δ −13 assignable to the phosphorus atoms of the chelated ligand. While the two phosphorus atoms of the chelate ligand are crystallographically distinct, examination of the $AgXP_3$ core geometries (Table 3, Fig. 2) suggests that the immediate chemical environment is similar for both atoms. Making the assumption that the chemical shifts of both of these atoms are the same, the ^{31}P NMR spectrum of each complex would be expected to consist of the A_2BM part of two overlapping A_2BMX spin systems which arise from spin–spin coupling to each of the two Ag spin ½ isotopes (^{107}Ag, 51.82%; ^{109}Ag, 48.18%). This multiplet pattern

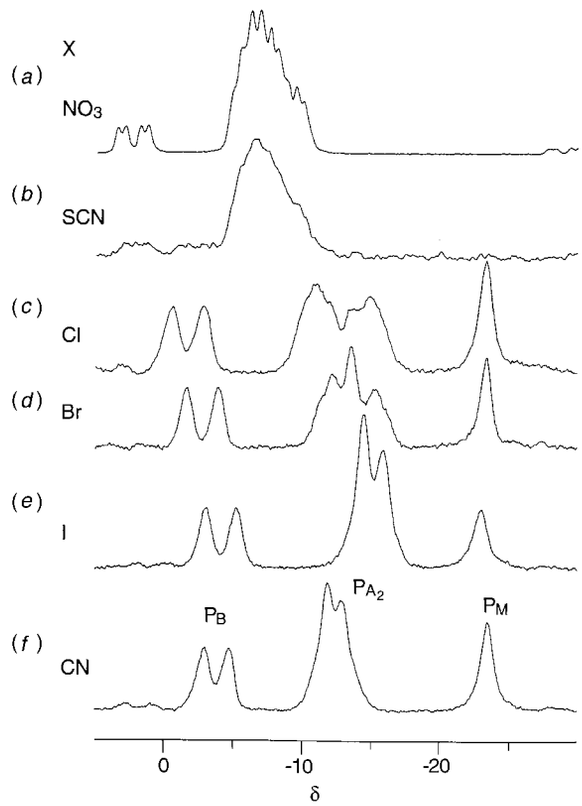

Fig. 3 The ^{31}P CP MAS spectra of $[Ag(dppp)_2]X$, (*a*) X = NO_3, (*b*) X = SCN and [AgX(dppp-*P*,*P*′)(dppp-*P*)] complexes, (*c*) X = Cl, (*d*) X = Br, (*e*) X = I and (*f*) X = CN. The neutral complexes are interpretable as A_2BMX spin systems (see text). In (*a*) the peaks at δ 0 to 5 are at present unassigned

can be assigned unambiguously in the ^{31}P solution spectrum of [AgBr(dppp-*P*,*P*′)(dppp-*P*)] (see below) and the solid-state spectra have the expected appearance of A_2BM multiplets in which the line widths are too broad (*ca.* 130 Hz) to resolve the multiplet splittings. The A_2BMX spin system is substantiated by two-dimensional ^{31}P CP MAS COSY spectra, as shown for [AgI(dppp-*P*,*P*′)(dppp-*P*)] in Fig. 4. The weak cross-peaks between the multiplets at δ −15 (P_{A_2}) and δ −4 (P_B) confirm that these resonances are part of the same spin system. No cross-peaks are observed between the high-field singlet (P_M) and the P_B multiplet, but the $^4J(P_B{-}P_M)$ coupling is expected to be only very small and was not resolved in the ^{31}P NMR solution spectrum of [AgBr(dppp-*P*,*P*′)(dppp-*P*)] (Table 5). The chemical shift of the high field singlet (P_M) is insensitive to the nature of the anion X in the four neutral complexes (Fig. 3) (and similar to the chemical shift of free dppp), consistent with the expected behaviour for the non-co-ordinated phosphorus environment in the unidentate dppp ligand. The relative broadness of the peak is consistent with the observed structural disorder about this atom (see above). Although the A_2BMX spin system is second order the ^2J(P–P) coupling constant is expected to be of the order of 50–80 Hz (*cf.* ref. 18), as shown for [AgBr(dppp-*P*,*P*′)(dpppO-*P*)] (Table 5). As this value is smaller than the line widths in the solid-state spectra, the observed line spacing of the low-field (P_B) doublet corresponds approximately to the value of $^1J(Ag{-}P_B)$. These values are tabulated in Table 4. Little change is observed in passing from the chloride to the bromide complexes. However, the value for the iodide decreases by *ca.* 5% while that of the cyanide decreases by a further 17%. These trends are consistent with those observed for the analogous series of complexes $[AgX\{P(C_6H_{11})_3\}_2]$[19] and reflect the similar donating properties of the halogens to silver in these complexes and, as expected, stronger Ag–X interactions in the cyanide complex. As for

Table 3 Molecular core geometries (distances in Å, angles in °) for [AgX(dppp-*P*,*P′*)(dppp-*P*)]

X	Cl	Br	I	CN[a]
Ag–X	2.567(5)	2.696(3)	2.852(1)	2.19(2)
Ag–P(1a)	2.508(5)	2.511(5)	2.494(2)	2.532(4)
Ag–P(2a)	2.512(4)	2.511(5)	2.514(2)	2.536(4)
Ag–P(1b)	2.438(5)	2.445(5)	2.437(3)	2.473(4)
X–Ag–P(1a)	105.7(2)	107.0(1)	107.66(6)	109.3(4)
X–Ag–P(2a)	103.3(2)	102.7(1)	101.66(5)	108.5(4)
X–Ag–P(1b)	104.9(2)	103.7(1)	103.61(5)	108.0(4)
P(1a)–Ag–P(2a)	93.1(1)	93.4(2)	93.68(7)	91.2(1)
P(1a)–Ag–P(1b)	123.2(2)	124.5(2)	125.74(7)	119.1(1)
P(2a)–Ag–P(1b)	124.1(1)	123.1(2)	121.88(1)	119.6(1)
Ag–P(1a)–C(1a)	108.3(5)	107.4(7)	107.7(3)	106.9(5)
Ag–P(2a)–C(2a)	106.7(5)	106.5(5)	106.5(2)	105.5(4)
P(1a)–C(1a)–C(12a)	117(1)	118(1)	117.8(5)	117.1(9)
P(2a)–C(2a)–C(12a)	114(1)	114(2)	114.3(5)	114.1(9)
C(1a)–C(12a)–C(2a)	115(1)	113(1)	116.4(6)	116(1)
Ag–P(1a)–C(111a)	118.0(7)	117.1(7)	116.5(3)	121.0(6)
Ag–P(1a)–C(121a)	120.6(7)	120.1(8)	121.2(3)	118.9(5)
Ag–P(2a)–C(211a)	117.7(5)	117.8(6)	119.1(2)	121.9(4)
Ag–P(2a)–C(221a)	125.2(5)	123.7(6)	122.4(2)	122.6(2)
Ag–P(1b)–C(111b)	115.5(6)	114.8(6)	115.0(3)	114.5(5)
Ag–P(1b)–C(121b)	113.3(5)	112.3(6)	113.7(2)	117.5(5)
C(1a)–P(1a)–C(111a)	105.8(8)	105.7(9)	105.0(4)	104.3(7)
C(1a)–P(1a)–C(121a)	98.6(8)	100.1(9)	99.9(3)	98.6(6)
C(2a)–P(2a)–C(211a)	98.7(7)	99.5(8)	100.4(3)	98.8(6)
C(2a)–P(2a)–C(221a)	102.6(7)	103.0(8)	104.1(4)	103.0(6)
C(1b)–P(1b)–C(111b)	102.4(7)	102.1(9)	102.4(3)	102.1(6)
C(1b)–P(1b)–C(121b)	104.8(7)	106.9(9)	105.9(3)	104.5(6)
C(2b)–P(2b)–C(211b)[b]	107(1)	106(1)	103.1(4)	104.6(9)
C(2b)–P(2b)–C(221b)[b]	98(1)	97(1)	98.9(4)	97.9(9)
C(111a)–P(1a)–C(121a)	103.2(9)	104(1)	104.2(4)	104.0(7)
C(211a)–P(2a)–C(221a)	101.8(7)	102.8(8)	101.4(3)	101.2(6)
C(111b)–P(1b)–C(121b)	103.6(7)	104.8(9)	103.4(3)	103.2(6)
C(211b)–P(2b)–C(221b)[b]	99(1)	98(1)	100.8(5)	100(1)
Ag–P(1a)–C(1a)–C(12a)	58(1)	59(1)	56.3(6)	60(1)
Ag–P(2a)–C(2a)–C(12a)	−64(1)	−64(1)	−63.3(5)	−66.7(9)
P(1a)–C(1a)–C(12a)–C(2a)	−79(2)	−81(2)	−77.6(8)	−78(1)
P(2a)–C(2a)–C(12a)–C(1a)	82(1)	83(2)	81.5(7)	82(1)
P(2a)–Ag–P(1a)–C(1a)	−38.6(5)	−37.7(7)	−37.8(3)	−42.6(5)
P(1a)–Ag–P(2a)–C(2a)	41.2(5)	41.3(6)	41.4(3)	45.4(5)
X–Ag–P(1a)–C(111a)	−173.9(6)	−174.6(6)	−176.7(3)	−173.6(7)
X–Ag–P(1a)–C(121a)	−46.1(8)	−46.5(8)	−48.2(3)	−42.8(7)
X–Ag–P(2a)–C(211a)	−175.4(5)	−177.6(6)	−179.9(3)	−176.5(7)
X–Ag–P(2a)–C(221a)	53.8(7)	51.6(8)	51.7(3)	51.7(7)
X–Ag–P(1b)–C(1b)	54.3(6)	55.5(7)	56.9(3)	51.8(7)
X–Ag–P(1b)–C(111b)	−65.4(6)	−62.5(7)	−61.8(2)	−64.7(6)
X–Ag–P(1b)–C(121b)	175.3(6)	177.9(7)	179.4(3)	173.9(7)
Ag–P(1a)–C(111a)–C(112a)	45(1)	44(2)	43.5(7)	45(1)
Ag–P(1a)–C(121a)–C(122a)	33(2)	35(2)	38.5(8)	28(1)
Ag–P(2a)–C(211a)–C(212a)	0(1)	1(2)	1.1(7)	1(1)
Ag–P(2a)–C(221a)–C(222a)	−97(1)	−98(2)	−99.9(6)	−95(1)
Ag–P(1b)–C(111b)–C(112b)	1(2)	0(2)	2.7(6)	−2(1)
Ag–P(1b)–C(121b)–C(122b)	60(1)	62(2)	61.1(6)	61(1)

[a] C–N 1.12(2) Å, Ag–C–N 179(1)°. [b] Major component.

Table 4 Solid-state CPMAS ^{31}P NMR parameters for [AgX(dppp-*P*,*P′*)(dppp-*P*)] complexes. Estimated error in coupling constants ±10 Hz

	δP_A	δP_B	δP_M	$^1J(P_B–Ag)$/Hz*
Cl	−12.8	−1.7	−23.3	363
Br	−13.6	−2.7	−23.4	367
I	−15.1	−4.1	−23.0	348
CN	−12.3	−3.8	−23.4	288

* Estimate only, based on multiplet splitting (Fig. 3). $^1J(P_B–Ag)$ is the average of the $^1J(^{109}Ag–^{31}P)$ and $^1J(^{107}Ag–^{31}P)$ coupling constants, see text.

the tricyclohexylphosphine complexes, the observed changes in the scalar coupling constants are not reflected in any significant changes in the Ag–P bond lengths for the halides, other than the small increase noted for the cyanide complex. The high-field multiplet corresponds to the two phosphorus nuclei in the chelated dppp ligand. The appearance of this multiplet is dependent on the nature of X (Fig. 3). For X = I or CN it consists of a broad, asymmetric doublet while for the bromide and chloride complex the spectrum devolves to a pair of overlapping doublets. A possible interpretation is that for X = I or CN the chemical shifts of the two chelated P are essentially the same in which case the observed splittings (*ca.* 232 and 173 Hz, respectively) will reflect the average $^1J(Ag–P_A)$ coupling constant. For X = Br or Cl the greater complexity of the multiplets suggests significant differences in different chemical shifts for the two phosphorus atoms. For X = Br the multiplet has the appearance of two overlapped doublets with a splitting of *ca.* 250 Hz. This agrees well with the estimate of the average value for $^1J(Ag–P_A)$ obtained from the ^{31}P solution spectrum of [AgBr(dppp-*P*,*P′*)(dppp-*P*)] (Table 5). However, for the Cl complex it

Table 5 Solution ^{31}P NMR parameters for 1:2 Ag:dppp complexes (estimated error in coupling constants ±1 Hz)

Compound	Solvent	T/K	δ P_A	δ P_B	δ P_M	$-^1J$/Hz P_A–^{107,109}Ag (average)	P_B–^{107,109}Ag (average)
[Ag(dppp)$_2$]X							
X = SCN[a]	$CDCl_3$	223	−4.7			221, 254 (237)	
[AgX(dppp-*P*,*P*′)(dppp-*P*)]							
X = Cl	$CDCl_3$	253	−7.9	*b*	−18.3	(250)[c]	*b*
X = Br	$CDCl_3$	223	−7.4[d]	−3.3[d]	−18.4	239, 276 (257)[d]	348, 402 (375)[d]
X = I	CD_2Cl_2–CH_2Cl_2	233	−11.8	*b*	−18.6	(250)[c]	*b*
X = CN (species I)	CD_2Cl_2–CH_2Cl_2	183	−12.4	−3.5	−20.8	(214)[c]	(245)[c]
X = CN (species II)	CD_2Cl_2–CH_2Cl_2	183	−13.0[e]	−2.7[e]	−19.6	*e*	*e*
[AgBr(dppp-*P*,*P*′)(dpppO-*P*)][f]	$CDCl_3$	223	−9.1	1.8	35.0	239, 276 (257)	348, 402 (375)

[a] The $[Ag(dppp)_2]^+$ cation is observed also as a dissociation product in solutions of [AgX(dppp-*P*,*P*′)(dppp-*P*)] (X = Cl, Br, I or CN) (see text). In $CDCl_3$ δ has a temperature dependence of −0.01 ppm K^{-1}. In CD_2Cl_2–CH_2Cl_2 δ is −5.3 at 233 K. [b] Overlapped by major doublet of doublets for $[Ag(dppp)_2]^+$. [c] Couplings not fully resolved at this temperature. [d] The P_A and P_B multiplets are partially obscured by the $[Ag(dppp)_2]^+$ resonance at δ −4.7 and also for P_A the [AgBr(dppp-*P*,*P*′)(dpppO-*P*)] multiplet at δ −9.1 [see Fig. 5(*e*)]. The chemical shifts are estimated based on the assumption that the coupling constants and the multiplet splitting patterns are identical to the analogous multiplets in [AgBr(dppp-*P*,*P*′)(dpppO-*P*)]. The spectrum simulated with these values gives a reasonable fit to the observed spectrum [Fig. 5(*e*)]. [e] Cannot be measured accurately due to overlap with compound I see Fig. 6. [f] $^2J(P_a–P_B) = 58$ Hz, $^4J(P_B–P_M) = 0$ Hz, $^6J(P_A–P_M) = 0$ Hz; see simulated spectrum Fig. 5(*e*).

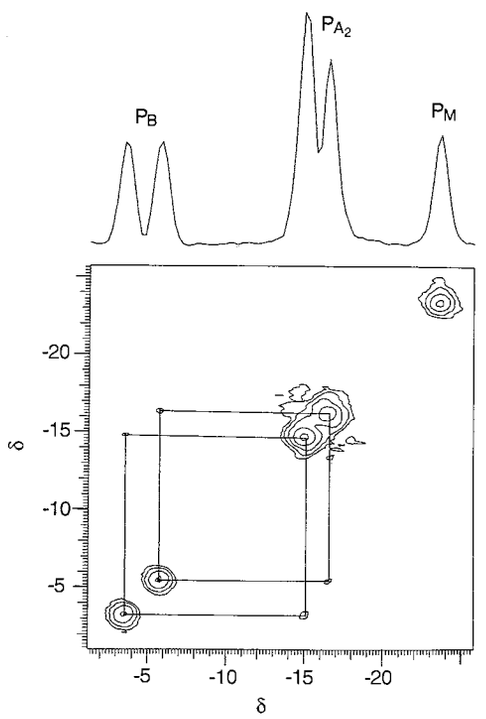

Fig. 4 The two-dimensional ^{31}P CP MAS COSY solid-state NMR spectrum of [AgI(dppp-*P*,*P*′)(dppp-*P*)]

is not possible to obtain an estimate of the value of $^1J(Ag–P_A)$ by inspection.

Solution ^{31}P NMR studies

The results of the structural and solid-state NMR studies described above show that both cationic $[Ag(dppp)_2]^+$ and neutral [AgX(dppp-*P*,*P*′)(dppp-*P*)] complexes can be isolated in the solid state with the formation of each dependent on the anion. To investigate which of these structures is favoured in solution, or whether an equilibrium exists between the two (Scheme 1), we recorded variable-temperature solution ^{31}P NMR spectra of the complexes in $CDCl_3$ and/or CD_2Cl_2–CH_2Cl_2 solutions. Representative spectra are shown in Fig. 5. For $[Ag(dppp)_2]$SCN in $CDCl_3$ a broad ($\Delta\nu_{\frac{1}{2}} = 350$ Hz) ^{31}P resonance (δ −5.9) was observed at 297 K which resolved below 273 K into two overlapping doublets (δ −5.1) characteristic of the $[Ag(dppp)_2]^+$ cation.[7] The $^1J(^{107,109}Ag–^{31}P)$ coupling constants (221 and 254 Hz) are the same as reported previously[7] for $[Ag(dppp)_2]NO_3$ although for the nitrate complex the spin–spin

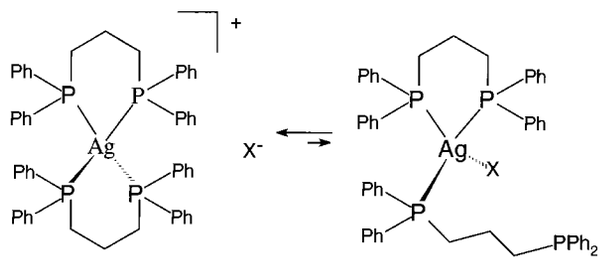

Scheme 1

couplings are resolved at 295 K. This is consistent with the relative donor strengths of the two anions, as the more weakly co-ordinating nitrate group would be less expected to facilitate rupture of the Ag–P bonds than the thiocyanate.

The ^{31}P solution spectra obtained from dissolution of the neutral [AgX(dppp-*P*,*P*′)(dppp-*P*)] complexes were found to be very dependent on the nature of X. For X = Cl in $CDCl_3$, the spectra exhibit a similar behaviour to the SCN complex. A broad ($\Delta\nu_{\frac{1}{2}} = 200$ Hz) resonance (δ −6.4) at 297 K resolved at 253 K into the two overlapping doublets for $[Ag(dppp)_2]^+$ [Fig. 5(*a*)]. However, unlike the SCN spectra, additional very minor signals were also just visible at this temperature. These had the expected multiplet pattern for [AgCl(dppp-*P*,*P*′)-(dppp-*P*)], with the assumption that the P_B multiplet was obscured by the major $[Ag(dppp)_2]^+$ resonance (Table 5). The total integrated intensity of these minor peaks was *ca.* 2% of the intensity of the $[Ag(dppp)_2]^+$ ^{31}P signals. This result shows that for the chloride complex in $CDCl_3$ solution, the equilibrium (Scheme 1) exists, but that the equilibrium constant lies well to the left, favouring displacement of the anion by the phosphine ligand.

An explanation for the exclusive formation of the neutral species in the solid state is that while the cation is the more stable species in solution, the neutral species is more stable in the solid state and preferentially forms under the recrystallization conditions necessary for the preparation of X-ray quality crystals.

For X = Br in $CDCl_3$ the ^{31}P NMR spectrum at 297 K consisted of a broad singlet (δ −7.5, $\Delta\nu_{\frac{1}{2}} = 200$ Hz). At 253 K this had partially resolved into the pair of doublets indicative of $[Ag(dppp)_2]^+$, together with a range of minor broad peaks between δ +6 and −10. All couplings were fully resolved on cooling the sample to 223 K [Fig. 5(*b*) and 5(*e*)]. The minor peaks arise from two distinct pairs of A_2BMX spin systems (for each of the ^{109}Ag and ^{107}Ag isotopes) which are assignable to

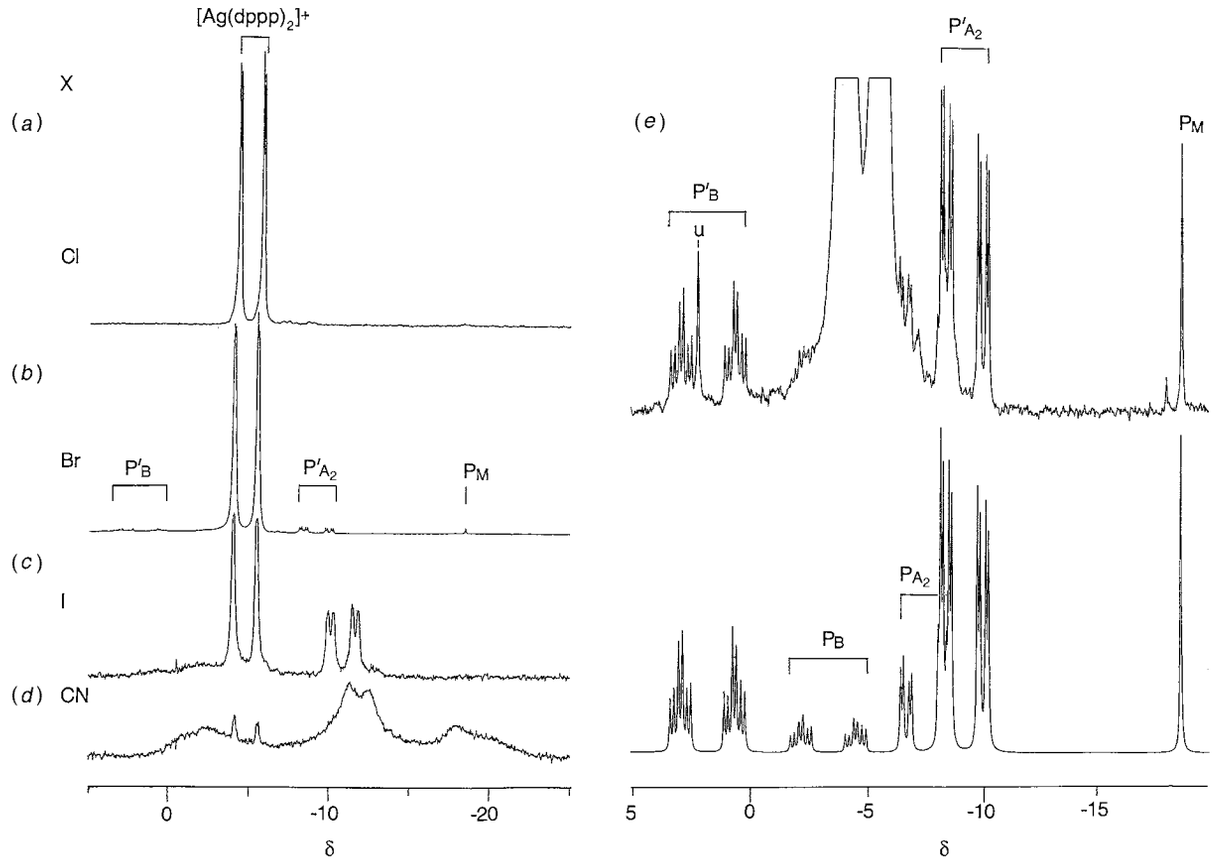

Fig. 5 Solution ^{31}P NMR spectra of [Ag(dppp)$_2$X] complexes in $CDCl_3$ at 223 K. (*a*) X = Cl (253 K), (*b*) X = Br, (*c*) X = I and (*d*) X = CN. (*e*) An expansion of spectrum (*b*) together with the simulated spectrum analysed as two distinct pairs of overlapping A_2BMX spin systems for each of the ^{109}Ag and ^{107}Ag isotopes. Peaks labelled P_{A_2}, P_B and P_M correspond to [AgBr(dppp-*P*,*P*′)(dppp-*P*)] and P'_{A_2} and P'_B to the oxidized species [AgBr(dppp-*P*,*P*′)(dpppO-*P*)]; the P'_M peak (not shown) is at δ +35 (see text). The derived chemical shifts and couplings constants for [AgBr(dppp-*P*,*P*′)(dpppO-*P*)] are given in Table 5. As the P_{A_2} and P_B multiplets for [AgBr(dppp-*P*,*P*′)(dppp-*P*)] are partially obscured by the $[Ag(dppp)_2]^+$ resonance, the simulated spectrum was obtained by estimating the chemical shifts of the two multiplets and assuming all coupling constants were the same as for the oxidized species. The peak labelled u is unidentified

[AgBr(dppp-*P*,*P*′)(dppp-*P*)] and, as well, its oxidation product [AgBr(dppp-*P*,*P*′)(dpppO-*P*)] in which the non-co-ordinated P in the unidentate dppp ligand has been oxidized. There was no evidence for oxidized product in the ^{31}P CP MAS spectrum of [AgBr(dppp-*P*,*P*′)(dppp-*P*)], suggesting that oxidation had occurred in solution in the period between preparation of the samples and acquisition of the spectra. Fig. 5(*e*) shows a comparison of the observed ^{31}P spectrum at 223 K, together with a simulated spectrum of two overlapped A_2BMX spin systems. From this we deduced that the well resolved multiplets [labelled P'_B and P'_{A_2}, Fig. 5(*e*)] are due to the chelated (P_{A_2}) and unidentate (P_B) phosphorus atoms in the oxidized species since the intensity of the signal at δ −18.4 is too low to correspond to the P_M resonance in the same spin system. A signal with the correct intensity for the oxidized P in [AgBr(dppp-*P*,*P*′)(dpppO-*P*)] was present at δ +35.0. The A_2 and B multiplets of [AgBr(dppp-*P*,*P*′)(dppp-*P*)] are partially obscured by the $[Ag(dppp)_2]^+$ ^{31}P signal, but are just visible in Fig. 5(*e*). These have the correct intensity to belong to the same pair of A_2BMX spin systems as the P_M signal at δ −18.4, as shown in the simulated spectrum. The chemical shifts and coupling constants derived from the simulated spectra are listed in Table 5. From peak integrals we estimate that the ring-opened species account for *ca.* 7% of the species present {[AgBr(dppp-*P*,*P*′)(dppp-*P*)] 2% and [AgBr(dppp-*P*,*P*′)(dpppO-*P*)] 5%}. This is slightly greater than for the chloride complex, reflecting a relative donor strength $Br^- > Cl^-$. However direct comparison is difficult since the equilibrium (Scheme 1) becomes irreversible once the unco-ordinated P is oxidized. When the sample of [AgBr(dppp-*P*,*P*′)(dppp-*P*)] was dissolved in CD_2Cl_2–CH_2Cl_2 the bis-chelated complex was the only species observed in the ^{31}P solution spectrum at 23 K.

For X = I in $CDCl_3$ the compound was not completely soluble at 297 K. However, a single ^{31}P resonance was observed which was sharper ($\Delta\nu_{\frac{1}{2}} = 130$ Hz) and more shielded (δ −9.2) than for the SCN, Cl and Br complexes indicating the occurrence of equilibria between different types of Ag^I phosphine species. As the solution was cooled the resonance broadened and then at 253 K began to resolve into three set of peaks: two broad doublets at δ −0.4 and −11.2, ^1J(Ag–P) (average) *ca.* 380 and 243 Hz, respectively and a very broad resonance at δ −6.8. At 223 K these resonances had been replaced by a pair of doublets centred at δ −10.8 [^1J(Ag–P) *ca.* 249 Hz, Fig. 5(*c*)] and a broadened doublet at δ −4.7 characteristic of $[Ag(dppp)_2]^+$. The ^{107,109}Ag–^{31}P couplings were not resolved above the freezing point of the solvent. No peaks were visible that were assignable to the ring-opened species [AgI(dppp-*P*,*P*′)(dppp-*P*)] but broadened resonances were observed in the region δ 0 to −4, indicative of additional species involved in exchange equilibria. In an attempt to identify the species present in solution we recorded ^{31}P NMR spectra of [AgI(dppp-*P*,*P*′)(dppp-*P*)] in CH_2Cl_2–CD_2Cl_2 since this allowed spectra to be obtained at lower temperatures. However, different behaviour was observed in this solvent and at 243 K the spectrum resembled that of the chloride complex with the two overlapping doublets characteristic of the $[Ag(dppp)_2]^+$ cation and additional minor signals with the expected multiplet pattern for [AgI(dppp-*P*,*P*′)(dppp-*P*)] (Table 5). There was a significantly greater proportion of the ring-opened species (*ca.* 16% of the total products, based on peak integrals) compared to the Br

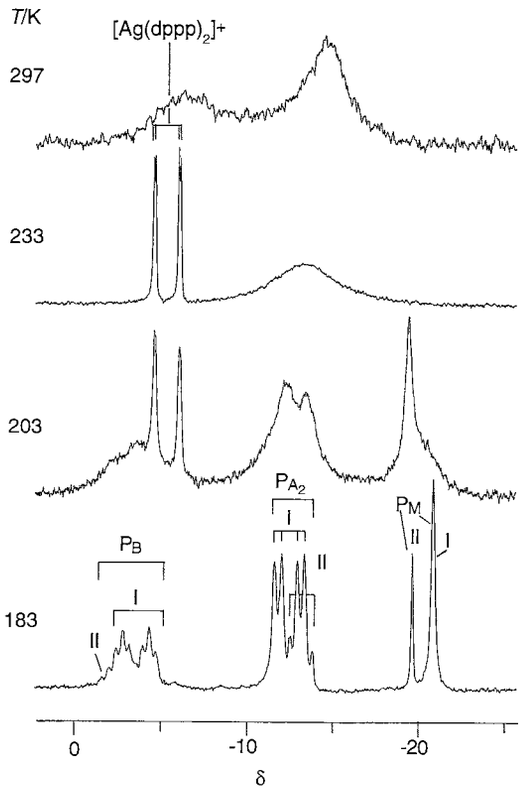

Fig. 6 Solution ^{31}P NMR spectra of [AgCN(dppp-*P*,*P*′)(dppp-*P*)] (4 mmol dm^{-3}) in CH_2Cl_2–30% CD_2Cl_2 at 297, 233, 203 and 183 K. The spectrum at 183 K is assignable as two independent A_2BMX spin systems which may arise from two different conformational structures (I and II) (see text and Table 5)

and Cl complexes consistent with the greater donor strength of I^-.

The ^{31}P NMR solution spectrum of the cyanide complex in $CDCl_3$ at 297 K was similar to the iodide complex with a single relatively sharp peak ($\Delta\nu_{\frac{1}{2}} = 140$ Hz) at δ −10.3. On cooling to 263 K, this resolved into a minor broad signal (δ −5.5) and a major signal (δ −11.1). At 233 K the former had resolved into the typical doublet for $[Ag(dppp)_2]^+$ (δ −4.9) and a major very broad peak (δ −12.1). With further cooling the latter separated into three broad resonances (δ −3, −11 and −18) [Fig. 5(*d*)]. The $[Ag(dppp)_2]^+$ ion accounted for only *ca.* 9% of the total products in solution, based on peak integrals. The temperature-dependent behaviour is consistent with the equilibrium (Scheme 1), in which there is little dissociation of the anion, so that the major species is [AgCN(dppp-*P*,*P*′)(dppp-*P*)]. However, the broadness of the peaks at 223 K is indicative of the occurrence of an additional equilibrium at low temperature. To investigate this further we recorded ^{31}P solution spectra of the complex in CH_2Cl_2–CD_2Cl_2 (Fig. 6). The rate of exchange was slower in this solvent so that at ambient temperature two broad resonances were observed (δ *ca.* −6.3 and −14.5). On cooling the low-field resonance resolved into the $[Ag(dppp)_2]^+$ pair of doublets with spin–spin couplings fully resolved at 233 K. This species accounted for *ca.* 38% of the total products at 273 K, but on cooling the intensity gradually decreased until the resonance disappeared altogether just below 193 K. The high-field resonance sharpened initially, then below 273 K broadened and shifted to high frequency. Below 233 K it began to resolve into three broad resonances (δ *ca.* −3, −13 and −19) and as the solution was cooled further these resolved into distinct sets of multiplets. Although the spin–spin couplings were not fully resolved above the freezing point of the solvent the spectrum at 183 K is interpretable as two distinct (but overlapped) A_2BMX spin systems. This is seen most clearly for the P_M resonance which shows two distinct singlets (δ −20.8 and −19.6) with an intensity ratio of 3:1; multiplets with the correct intensity ratio for the second A_2BMX spin system are visible, although partially overlapped with the major P_{A_2} and P_B multiplets. The chemical shifts and coupling constants for the two A_2BMX spin systems are listed in Table 5. Although the $^1J(P_B–Ag)$ and $^1J(P_B–Ag)$ coupling constants of the major species are slightly larger than estimated from the ^{31}P CP MAS spectrum of [AgCN(dppp-*P*,*P*′)(dppp-*P*)] the chemical shifts for the three non-equivalent P environments are similar to those observed in the solid state and it seems reasonable that each of the species observed in solution is [AgCN-(dppp-*P*,*P*′)(dppp-*P*)] with, however, the substituents on the dppp ligands frozen into two distinct conformational structures.

Conclusion

Structural dislocation is observed in complexes of 1:2 AgX:dppp stoichiometry which can be isolated in both cationic $[Ag(dppp)_2]X$ and neutral [AgX(dppp-*P*,*P*′)(dppp-*P*)] forms in the solid state, depending on the anion X. To date, the neutral form only has been isolated from acetonitrile for X = Cl, Br, I or CN, whereas for SCN^- and NO_3^- the cationic complex only is isolated. In solution, the two forms exist in an equilibrium involving displacement of the anion by the uncoordinated phosphine ligand. For Cl^- the cationic form is favoured almost exclusively, consistent with the results of previous studies[1,4] on the related complexes $[Ag(dppe)_2]NO_3$ and $[Ag(eppe)_2]NO_3$ which showed that Cl^- does not readily displace P from the Ag co-ordination sphere. For the bromide complex similar behaviour was observed although the observation of significant amounts of ring-opened phosphine oxide complex [AgBr(dppp-*P*,*P*′)(dpppO-*P*)] in chloroform solution highlights the ease of opening of the chelated diphosphine, and subsequent oxidation, in the presence of the co-ordinating anion. For X = I, a greater proportion of the neutral complex exists in solution, consistent with the increased donor strength of I^-, and competing dissociative equilibria are also evident in $CDCl_3$ solutions. For X = CN, the neutral complex is favoured, with little formation of the cationic complex. Since the antitumour properties of metal diphosphine complexes may be related to the uptake of lipophilic cations into mitochondria, studies of this type are of fundamental importance to a meaningful interpretation of structure–activity relationships to establish whether the bis-chelated cationic species $[Ag(dppp)_2]^+$ will be the major species present *in vivo* for the different complexes of 1:2 AgX:dppp stoichiometry.

Acknowledgements

We acknowledge support of this work by the Australian Research Council and the Australian National Health and Medical Research Council (R. Douglas Wright Award to S. J. B.-P.). We thank Dr. David Rice (Varian, Palo Alto) for assistance with the two-dimensional CP MAS COSY pulse sequence.

References

1 S. J. Berners-Price, R. K. Johnson, A. J. Giovenella, L. F. Faucette, C. K. Mirabelli and P. J. Sadler, *J. Inorg. Biochem.*, 1988, **33**, 285.
2 S. J. Berners-Price and P. J. Sadler, *Struct. Bonding* (*Berlin*), 1988, **70**, 28.
3 S. J. Berners-Price and P. J. Sadler, *Coord. Chem. Rev.*, 1996, **151**, 1.
4 S. J. Berners-Price, D. C. Collier, M. A. Mazid, P. J. Sadler, R. E. Sue and D. Wilkie, *Metal-Based Drugs*, 1995, **2**, 111.
5 P. Di Bernardo, G. Dolcetti, R. Portanova, M. Tolazzi, G. Tomat and P. Zanonato, *Inorg. Chem.*, 1990, **29**, 2859.
6 A. Del Zotto, P. Di Bernardo, M. Tolazzi, G. Tomat and P. Zanonato, *J. Chem. Soc., Dalton Trans.*, 1993, 3009.

7 S. J. Berners-Price, C. Brevard, A. Pagelot and P. J. Sadler, *Inorg. Chem.*, 1985, **24**, 4278.
8 Effendy and A. H. White, unpublished work.
9 S. R. Hall, H. D. Flack and J. M. Stewart, *The XTAL 3.2 Reference Manual*, Universities of Western Australia, Geneva and Maryland, 1992.
10 F. J. Blount, D. Camp, R. D. Hart, P. C. Healy, B. W. Skelton and A. H. White, *Aust. J. Chem.*, 1994, **47**, 1631.
11 G. Wu and R. E. Wasylishen, *Organometallics*, 1992, **11**, 3242.
12 C. S. W. Harker and E. R. T. Tiekink, *J. Coord. Chem.*, 1990, **21**, 287.
13 C. Franzoni, G. Pelizzi, G. Predieri, P. Tarasconi and C. Pelizzi, *Inorg. Chim. Acta*, 1988, **150**, 279.
14 M. C. Gimeno, P. G. Jones, A. Laguna and C. Sarroca, *J. Chem. Soc., Dalton Trans.*, 1995, 1473.
15 J. F. Dobson, B. E. Green, P. C. Healy, C. H. L. Kennard, C. Pakawatchai and A. H. White, *Aust. J. Chem.*, 1984, **37**, 649.
16 P. F. Barron, J. C. Dyason, P. C. Healy, L. M. Engelhardt, B. W. Skelton and A. H. White, *J. Chem. Soc., Dalton Trans.*, 1986, 1965.
17 L. M. Engelhardt, P. C. Healy, V. A. Patrick and A. H. White, *Aust. J. Chem.*, 1987, **40**, 1873.
18 S. Attar, N. W. Alcock, G. A. Bowmaker, J. S. Frye, W. H. Bearden and J. H. Nelson, *Inorg. Chem.*, 1991, **30**, 4166.
19 G. A. Bowmaker, Effendy, P. J. Harvey, P. C. Healy, B. W. Skelton and A. H. White, *J. Chem. Soc., Dalton Trans.*, 1996, 2449.

Received 12*th November* 1996; *Paper* 6/07692K